ACS Sustainable Chemistry & Engineering

Research Article

pubs.acs.org/journal/ascecg

Attapulgite/Poly(acrylic acid) Nanocomposite (ATP/PAA) Hydrogels with Multifunctionalized Attapulgite (org-ATP) Nanorods as Unique Cross-linker: Preparation Optimization and Selective Adsorption of Pb(II) Ion

Peng Liu,[†,*] Liping Jiang,[†,‡] Longxiang Zhu,[†] and Aiqin Wang[§]

[†]State Key Laboratory of Applied Organic Chemistry, Institute of Polymer Science and Engineering, College of Chemistry and Chemical Engineering, Lanzhou University, Lanzhou 730000, China

[‡]Department of Chemistry, Gansu Lianhe University, Lanzhou 730000, China

[§]Center of Xuyi Attapulgite Applied Technology,, Lanzhou Institute of Chemical Physics, Chinese Academy of Science, Lanzhou 730000, China

S *Supporting Information*

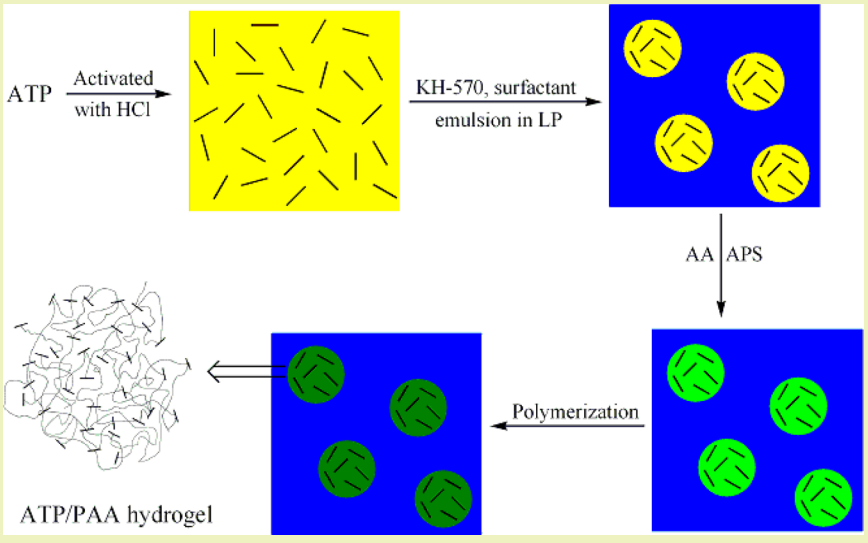

ABSTRACT: A facile strategy is developed to synthesize the novel attapulgite/poly(acrylic acid) nanocomposite (ATP/PAA) hydrogels via the "one-pot" inverse suspension polymerization with the multifunctionalized attapulgite (org-ATP) as the unique cross-linker. The org-ATP is in situ produced directly in the form of water-in-oil emulsion and then used as prepared for the inverse suspension polymerization without being separated; so the proposed strategy is much simpler compared with the traditional methods. Almost all acrylic acid (AA) monomers have been successfully grafted onto ATP to form the 3-dimensional cross-linking network of the nanocomposite hydrogels, in which the org-ATP nanorods, as cross-linker and structural strengthening agent, drastically improves the mechanical stability of the resulting ATP/PAA hydrogels. The nanocomposite hydrogels exhibit selective adsorption toward the Pb(II) ion with a maximum adsorption capacity of 42 mg/g, and the adsorbed Pb(II) ion could be eluted completely. The optimized nanocomposite hydrogel adsorbent also exhibits an excellent reusability. The adsorption capacity and desorption rate remain unchanged for at least 10 cycles of adsorption−desorption. These strong points make it a potential adsorbent for heavy metal-contaminated water.

KEYWORDS: *Nanocomposite hydrogels, Cross-linker, "One-pot" inverse suspension polymerization, 3-Dimensional cross-linking network, Selective adsorbent, Heavy metal*

INTRODUCTION

Heavy metals in a water environment mainly come from industrial waste disposals, and they could spread easily due to the fluidity and permeability of water. They have resulted in severe and uncontrollable environmental damages because they

Received: August 29, 2013
Revised: December 9, 2013
Published: December 12, 2013

hardly degrade naturally and may gradually propagate and accumulate in an organism's body through the food chain.

The widely used water treatment techniques are commonly used for certain processes, including chemical precipitation, physical adsorption, chemical adsorption, ion exchange, extraction, or biological treatment.[1,2] Among them, chemical precipitation and physical adsorption are not very effective for treating wastewater containing heavy metals at low concentration. Ion exchange and extraction have the problem of secondary contamination, and biological treatment is not widely applicable. Chemical adsorption has exhibited many advantages, such as mild adsorption conditions, broad range adaptability, and excellent adsorption effectiveness. By now, the polymeric ion-exchangers and chelating resins are the most used chemical adsorbents for heavy metal ions.[3]

With the development of nanoscience and nanotechnology, it is realized that polymer performances (mechanical stability, etc.) could be improved dramatically by introducing nanomaterials to form various polymer-based nanocomposites.[4−7] Recently, many inorganic/polymer nanocomposites had been prepared as adsorbents of heavy metal ions.[8] In most of the reported inorganic/polymer nanocomposite adsorbents, the inorganic nanomaterials were mixed into the cross-linked polymers without covalent bonding, via physical blending,[9−15] or intercalation.[16]

Introducing covalent bonds between the inorganic nanomaterials and the cross-linked polymers is expected to produce improved strength and stability. The functional polymers have been grafted onto various nanomaterials, such as silica nanoparticles,[17,18] carbon nanotubes,[19] and attapulgite,[20−22] as the nanosized adsorbents for the removal of heavy metal ions from wastewaters. However, their practical applications have been restricted due to difficult separation, except for those based on magnetic nanoparticles.[23−26]

Most recently, Zhao and Cao developed a facile method to prepare adsorbent with three-dimensional interpenetrating network structures for Pb(II) ions via emulsion copolymerization of acrylonitrile, γ-methacryloxypropyl trimethoxy silane (KH-570), and N,N′-methylene-bis-acrylamide (MBA), followed with hydrolysis of silane to form silica quantum dots.[27] The silica/polyacrylonitrile nanospheres obtained were chemically cross-linked via both the cross-linker MBA and silica quantum dots formed.

In the present work, the advantages of clay nanomaterials and functional polymers were combined to develop a low-cost chemical adsorbent with a high mechanical property for industrial water treatment. The most inexpensive natural nanorods of attapulgite (ATP) were surface-modified to be used as not only the structural strengthening agent but also the cross-linker for the linear poly(acrylic acid) (PAA). So the clay/polymer nanocomposite hydrogel adsorbents were synthesized via inverse suspension polymerization without any conventional cross-linker added (Scheme 1). In the proposed strategy, the ATP nanorods were in situ modified with KH-570 in liquid paraffin (LP), and the dispersion of the multifunctional attapulgite (org-ATP) nanorods were used directly for the inverse suspension polymerization of AA without being separated. The preparation condition of the novel attapulgite/poly(acrylic acid) nanocomposite (ATP/PAA) hydrogels was optimized for the adsorbent toward heavy metal ions. The swelling ratio and mechanical stability of the ATP/PAA hydrogels were also discussed.

Scheme 1. Schematic Illustration of Preparation Route for ATP/PAA Nanocomposite Hydrogel Adsorbent

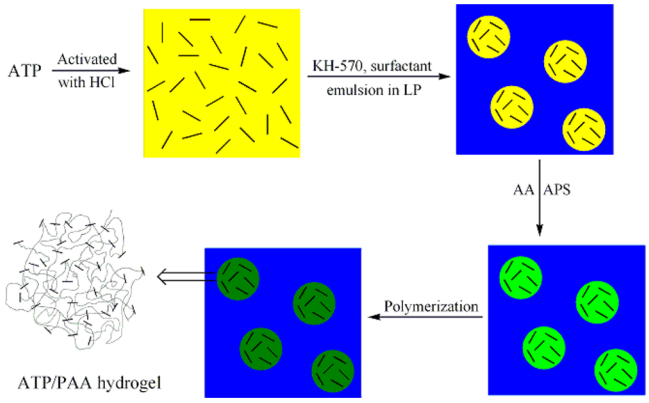

EXPERIMENTAL METHODS

Materials. The ATP mineral was provided by the R&D Center of Xuyi Attapulgite Applied Technology, Lanzhou Institute of Chemical Physics, CAS.

Acrylic acid (AA) was provided by Tianjin Kaixin Chemical Industry Co., Ltd., China. Tween-60, Span-80, and liquid paraffin were provided by Tianjin Guangfu Fine Chemical Research Institute, China. KH-570 was provided by Jiangsu Chenguang Silane Co., Ltd., China. Ammonium persulfate (APS), hydrochloric acid (HCl), and other reagents used were all analytical-reagent grade. Deionized water was used throughout the experiments.

Synthesis of Org-ATP. The ATP mineral was first baked to remove organic compounds in order to prevent interference with the graft polymerization. Then it was grinded in water with a high-speed dispersion machine at 4000 rpm for 4 h until being dispersed uniformly in the nanorod state. It was then treated with 0.10 mol/L HCl to activate its surface to get an activated ATP (AATP) aqueous dispersion, whose solid content could be controlled in the range of 15−25%.

The AATP dispersion was added into liquid paraffin (LP) with the mixture of Span-80 and Tween-60 as emulsifiers at a given oil−water ratio, stirred for 0.5 h, and then KH-570 (weight ratio to AATP was 1:3) was added. After the mixture was stirred for 0.5 h, it was heated to 60 °C and stirred for 6 h at the temperature. The feeding amounts for the org-ATP were summarized in Table 1.

Table 1. Formulation for org-ATP Dispersion

materials	amount (g)
AATP dispersion (solid content: 21%)	10.0
liquid paraffin	30.0
Span-80	0.35
Tween-60	0.15
KH-570	0.70

Synthesis of ATP/PAA Hydrogels. *Preparation Process.* Certain amounts of Span-80, Tween-60, and LP were added into a Wolff bottle, and the mixture was stirred for 0.5 h. Then AA was added at formula ratio, and the mixture was stirred for 1 h. After a given amount of AATP dispersion and APS was added, the mixture was stirred for 0.5 h and maintained at 60 °C with stirring for 2 h, followed by 80 °C for 3 h under N_2 atmosphere.

The ATP/PAA hydrogels were separated from LP and washed with ether, ethanol, and water in sequence. Finally, they were immersed in an ammonia solution at pH 8−9 three times for 24 h each time, followed by extraction in water for 24 h to remove the free ungrafted PAA. The resulting products were dried in vacuum.

Orthogonal Experiment. On the basis of the previous experimental results, the effects of the feeding ratio of the AATP nanorods to AA

dx.doi.org/10.1021/sc400321v | ACS Sustainable Chem. Eng. 2014, 2, 643−651

(AATP/AA), ratio of Span-80 and Tween-60 (Span-80/Tween-60), amount of initiator (APS), oil–water ratio, and stirring rate on the products were investigated with an orthogonal experiment (Table S1, Supporting Information).[28]

Single Factor Experiment. A single factor experiment was designed to investigate the effect of the mass ratio of AATP to AA on the properties of the products (Table S2, Supporting Information) based on the results of the orthogonal experiment.

Water Absorption Ratio. The weighted dry sample was immersed into water for 24 h. The swollen sample was weighed after the surface water was wiped with filter paper. The water absorption ratios were expressed by the mass ratio of the absorbed water to the dry samples.

Volume Expansion Ratio. The length and diameter of the dried and swollen ATP/PAA hydrogels were measured with a spiral micrometer. The volume expansion ratio is expressed by the average growth multiples of the lengths (ΔD_l) and diameters (ΔD_d).

Mechanical Stability Testing. The mechanical stability of the ATP/PAA hydrogels was investigated by testing their resistance to pressure or shear flows. After the ATP/PAA hydrogels were immersed in water for 24 h, they were stirred with a high-speed agitator at 2000 rpm for 2 h. The damage rates of the ATP/PAA hydrogels were investigated to evaluate their antishearing ability.

Their pressure resistance capability was tested by being loaded with 2.0 kg after being swollen for 24 h. The load bearings of the swollen ATP/PAA hydrogels were used to estimate their pressure resistances.

Adsorption Performance. The adsorption properties to heavy metal ions were investigated by a 180-80 polarized Zeeman-effect background-corrected flame atomic absorption spectrometer (FAAS) equipped with a Model 056 recorder. All the data presented were the averages of at least three time measurements with relative standard deviations of <3%.

Accurately weighed ATP/PAA hydrogels of about 0.10 g was added into 50 mL of a 0.20 g/L Cu^{2+} solution at pH 5.63, and the mixture was stirred for 3 h. The concentrations of the remained Cu^{2+} were measured by FAAS to evaluate the adsorption capacity of the ATP/PAA hydrogels.

The accurately weighed ATP/PAA hydrogels of about 0.10 g were added into a 50 mL solution containing 5 mg of Pb^{2+}, Cd^{2+}, Zn^{2+}, Ni^{2+}, and Cu^{2+} ions and stirred for 3.0 h. The concentrations of the remaining ions were measured by FAAS to evaluate the adsorption capacity and the adsorption selectivity of the ATP/PAA hydrogels to the heavy metal ions.

After the ion-adsorbed ATP/PAA hydrogels were filtered with an air pump, washed with water, and the remaining solution was wiped off with filter paper, they were then put into 50 mL of a 1.0 mol/L HCl aqueous solution and stirred for 1 h. The concentrations of the eluted ions in the upper liquid were measured by FAAS to evaluate the desorption ratio.

Analysis and Characterization. Bruker IFS 66 v/s infrared spectrometer was used for the FT-IR analysis in the range of 400–4000 cm^{-1} with a resolution of 4 cm^{-1}. The KBr pellet technique was adopted.

Thermogravimetric analysis (TGA) was performed with a Perkin-Elmer TGA-7 system at a scan rate of 20 °C min^{-1} at 800 °C in N_2.

The morphologies of the AATP and org-ATP were characterized with a JEM-1200 EX/S transmission electron microscope (TEM). The AATP was dispersed ultrasonically in water for 30 min and then deposited on a copper grid covered with a perforated carbon film. The org-ATP was deposited on the copper grid directly from the reacting mixture.

After the swollen hydrogels were dried in a freeze-dryer and cut into halves, the surfaces of the samples were observed by scanning electron microscopy (SEM) on an S-4800 field emission scanning electron microscope operated at 5.0 kV.

RESULTS AND DISCUSSION

Organo-modification of ATP. Before the surface organo-modification of the AATP nanorods with the polymerizable groups, they were activated with acid to introduce more surface silanol groups, so that more polymerizable groups may be grafted onto the ATP nanorods, and the final org-ATP nanorods could act as the cross-linker in the nanocomposite hydrogels subsequently.[29−32]

In the previous works reported, the inorganic nanomaterials were usually modified by KH-570 in toluene,[20,33−36] ethanol,[37,38] THF,[39] or an ethanol–water mixture.[40] Different from those traditional methods, the surface modification of the AATP nanorods in the present work was conducted in liquid paraffin (LP). In addition, Span-80 and Tween-60 were used as the surfactants to make the AATP aqueous dispersion emulsify uniformly in LP, which increased the collision probability between the AATP nanorods in the water phase and KH-570 molecules in the oil phase. Therefore, KH-570 could be easily grafted onto AATP with the proposed approach.

The TGA result of the modified ATP nanorods (Figure 1, curve a) showed that the organic component content was as high as 19.4%. Furthermore, the TEM image of the modified ATP nanorods was similar to that of AATP (Figure 2). These indicated that hardly any KH-570 was hydrolyzed and self-polymerized in the new surface modification method developed in the present work. So the utilization of KH-570 was increased, and the material cost was lowered significantly. In addition, the water-in-oil emulsion of the org-ATP nanorods could be used in the following inverse suspension polymerization directly, without being separated, washed, dried, and redispersed. So the developed route is simple, low in cost, and environment friendly.

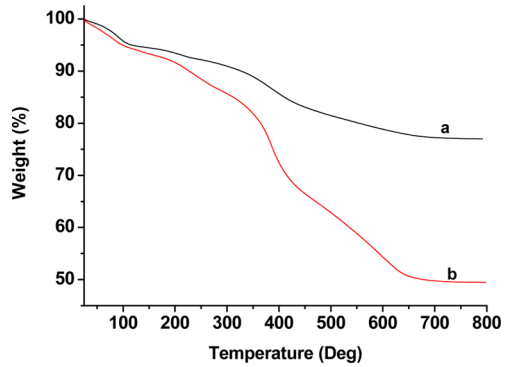

Figure 1. TGA curve of the org-ATP nanorods (a) and the residue separated from liquid paraffin after the inverse suspension polymerization (b).

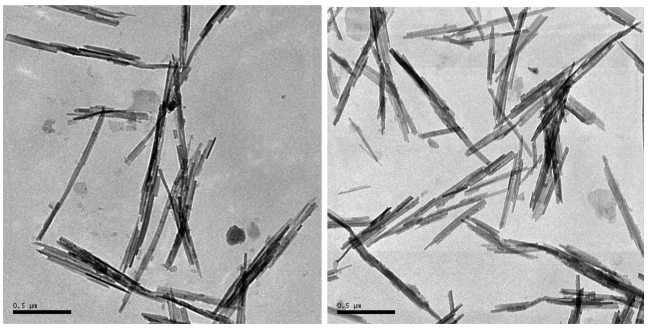

(a) (b)

Figure 2. TEM images of the AATP (a) and org-ATP nanorods (b). The scale bar is 0.5 μm.

dx.doi.org/10.1021/sc400321v | ACS Sustainable Chem. Eng. 2014, 2, 643−651

Synthesis of ATP/PAA Hydrogels. *Preliminarily Optimized Technical Conditions from Orthogonal Experiment.* The effects of experimental factors on the ATP/PAA hydrogels from the facile "one-pot" inverse suspension polymerization are summarized in Table S1 of the Supporting Information. One can see that the ATP/PAA hydrogels were obtained only in A2, A8, A11, and A13 under the oil−water ratio of 3:1. It indicates that the oil−water ratio plays the most important role in the preparation of the ATP/PAA hydrogels, and its optimized value was 3:1.

In addition, when the stirring rate was higher than 300 rpm, the produced turbulence made part of the sticky PAA splash around and stick seriously on the wall of reactor, which would reduce the final yield. Therefore, the stirring rate was controlled to 200−300 rpm.

Among the ATP/PAA hydrogels samples, the A2 sample had a small variation in diameter and a suitable size with a dried average diameter of about 1.5 mm. However the A8, A11, and A13 samples were bigger with average diameters of 2.8, 4.3, and 3.6 mm, respectively. Taking account the longer adsorption equilibrium time needed for the bigger gels toward heavy metal ions, the A2 sample was selected for the following single factor experiment.

This preliminarily optimized result was also verified by TGA analysis (Figure 3). It indicated that the grafting percentage

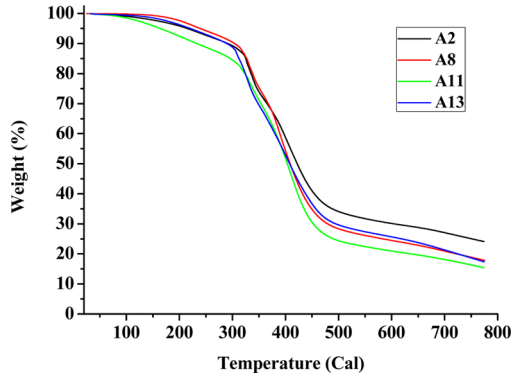

Figure 3. TGA curves of A2, A8, A11, and A13 samples.

(PG%, weight ratio between the polymer grafted and the ATP nanorods) of the A2, A8, A11, and A13 samples were 66.0%, 71.7%, 75.6%, and 70.4%, respectively. Compared to their theoretical values of 75.0%, 83.3%, 87.5%, and 90%, the PG% of A2 is the closest one to its theoretical value, namely, almost all the monomer AA in A2 had been copolymerized with the org-ATP nanorods to form the cross-linked hydrogels. Therefore, the A2 series was chosen for the single factor experiment.

Further Optimized Technical Conditions from the Single Factor Experiment. A series of formulations with different feeding ratios of AATP to AA were designed for the single factor experiment of the A2 series (Table S2, Supporting Information). It was found that the ATP/PAA hydrogels could be obtained under all formulas, except for the feeding ratio of AATP to AA of 1:1. The ATP/PAA hydrogels can deposit from liquid paraffin once after stirring was stopped, and the diameter of the ATP/PAA hydrogels increased with an increase in the feeding ratio of AA.

In addition, there is a catastrophic point between A2-4 and A2-5, namely, the upper LP layer of A-2 and A2-3 looked turbid. The upper layer of A2-4 was improved slightly but still turbid, while the LP layer from A2-5 to A2-9 looked transparent (Table S2, Supporting Information). After the same volume of water was added into the turbid LP and stirred, the suspended matter was still in the upper LP layer after being kept still for 10 min. This indicated that part of the org-ATP from A-2 to A2-4 failed to react with AA at the given ratio, and the unreacted org-ATP remained in LP and resulted in the turbidity of the upper LP layer. This was revealed by the TGA curve of the residue separated from LP (Figure 1, curve b). The weight loss of the residue was found to be about 20% in the temperature range of 300−500 °C. This was higher than the value of the org-ATP of <10% and lower than the values of the ATP/PAA hydrogels (50−60%). So it could be concluded that the org-ATP in the A2-5 to A2-9 were all incorporated into the composite hydrogels.

Analysis of ATP/PAA Hydrogels. *Water Absorption Ratio (A_w).* The water absorption ratios (A_w) of the ATP/PAA hydrogels after being immersed in deionized water for 24 h were summarized in Figure 4. The A_w increased with an

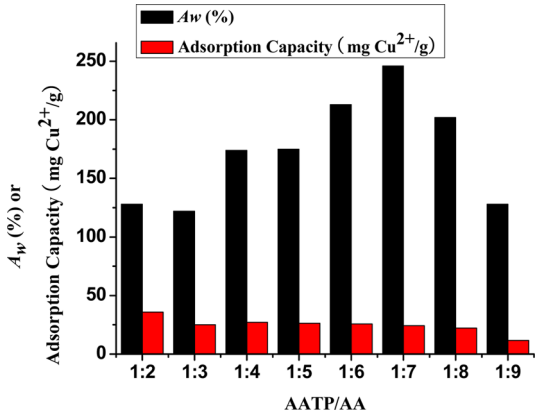

Figure 4. Effect of the AATP/AA feeding ratio on the water absorption ratios (A_w) and adsorption capacity toward Cu^{2+} of the resulting ATP/PAA hydrogels.

increase in AA, reaching the maximum at A2-7, and then decreased due to the three-dimensional (3-D) cross-linking network structure. The A_w is associated not only with the amount of hydrophilic groups[41] but also with cross-linking density of the 3-D network structure.[42] With a decrease in the feeding ratio of AATP/AA from 1:1 to 1:9, the cross-linking density of the 3-D network structure decreased. The grafted PAA was rich in the hydrophilic carboxyl group, which in turn hydrates with water molecules to expand the network chains. Meanwhile, the osmotic pressure resulted from the higher concentration of the carboxyl group inside the network promotes water molecules to permeate into the network.[43] In addition, the carboxyl groups inside the network repel with each other, leading to further expansion of the network.[44] Therefore, A_w increases with an increase in the content of the carboxyl groups, namely, with the rise of the concentration of AA until the ratio of AA to AATP of 7.

However, with the further rise of the concentration of AA, the cross-linking density decreases. As the cross-linking density reaches a certain level, the grid of the network is so small that it hinders the permeation of water molecules;[45] furthermore, the rise of the elastic shrinkage of the PAA chains has a negative effect on the permeation of the water molecules.[46] Therefore,

dx.doi.org/10.1021/sc400321v | ACS Sustainable Chem. Eng. 2014, 2, 643−651

A_w starts to decrease with a further increase in the feeding ratio of AA to AATP to 7.

Volume Expansion Ratio. The obtained ATP/PAA hydrogels appeared obvious to swelling in water (Table S3, Supporting Information). All the ATP/PAA hydrogels visually expanded after being immersed in water for 24 h. The products from A2-2 to A2-5 with the relatively higher AATP contents appear to be ellipsoidal shaped; however, with a decrease in the ATP content, PAA dominates the shape of the products,and the products from A-6 to A2-9 tend to be granular. The average growth multiples of the lengths (ΔD_l) and diameters (ΔD_d) of the dried and swollen ATP/PAA hydrogels were measured and are listed in Table S4 of the Supporting Information.

The data revealed that all samples expanded in the range of 120~250%. The ellipsoidal ATP/PAA hydrogels from A-2 to A2-5 are slightly different in length and diameter expansions. The average growth multiples of the lengths are slightly lower than those of the diameters, probably due to the orientation of the ATP nanorods with the lower PAA. When the ratio of AA to AATP increased further, the ATP/PAA hydrogels became biggr, and tended to be granular from A-6; the volume expansion reached the highest and then reduced in accordance with A_w (Figure 4).

Mechanical Stability. The anti-shearing ability and pressure resistance of the ATP/PAA hydrogels were used to evaluate their application stability. None of the ATP/PAA hydrogels was broken after being stirred at 5000 rpm for 2 h and showed no crack with a 2 kg load (Figure S1, Supporting Information). These experimental results verified that the ATP nanorods had enhanced the mechanical stability of the PAA network greatly, which increased the application stability and reproducibility of the ATP/PAA hydrogels. PAA was grafted onto ATP to form a cross-linking structure, where ATP worked as the cross-linking points (Scheme 1). The covalent linkages between the PAA matrix and ATP nanorods increased the flexural moduli and restricted the segmental motion of the PAA network,[47] which further improved their mechanical properties and dimensional stability significantly.[48−50]

Composition Analysis. TGA was used to evaluate the proportion of the grafted PAA in the A-2 series of the nanocomposite hydrogels (Figure 5). It revealed that the mass percent of the grafted PAA from A2-2 to A2-9 was 63.0%, 65.9%, 68.1%, 71.4%, 76.6%, 74.0%, 74.0%, and 75.4%, respectively. Compared to their theoretical values of 66.7%, 75.0%, 80.0%, 83.3%, 85.7%, 87.5%, 88.9%, and 90%, respectively, it could be concluded that more than 83% AA had been grafted onto the ATP nanorods in all the products from the A2 series.

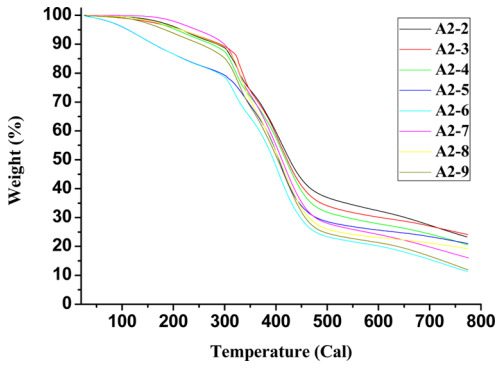

Figure 5. TGA curves of the samples in A2 series.

Preliminary Adsorption Testing. The Cu^{2+} ion was used to preliminarily test the adsorption property of the ATP/PAA hydrogels in the A2 series due to its color, as shown in Figure 4. The adsorption capacity of the ATP/PAA hydrogels toward Cu^{2+} ion deceased in the order of A2-2 to A2-9 due to their increased diameters. So the adsorption of the heavy metal ion on the surface of the ATP/PAA hydrogels increased, which could act as the ionic cross-linking agents to increase the elastic shrinkage of the polymer chains.[51] As a result, the further permeation of the heavy metal ions was hampered. On the other hand, the electrostatic repulsion between the metal ions on the surface and those in solution also has a negative impact on further adsorption.[52]

As previously described, part of the org-ATP did not react with AA from A-2 to A2-4. Meanwhile, the grafting ratio of PAA and the adsorption capacity of the ATP/PAA hydrogels toward the Cu^{2+} ion decreased in the order of A2-5 to A2-9. Considering the utilization of the raw materials and the production efficiency, A2-5 was selected as the optimal ATP/PAA nanocomposite hydrogel adsorbent.

Characterization of ATP/PAA Hydrogel A2-5. The FTIR spectra of the AATP, org-ATP, and ATP/PAA hydrogel A2-5 are compared in Figure 6. The absorbance peaks of

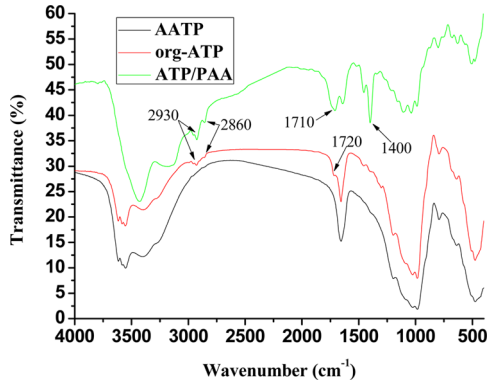

Figure 6. FTIR spectra of the AATP, org-ATP, and ATP/PAA hydrogels.

methyl and methylene groups around 2930 and 2860 cm^{-1} and that of C═O groups at 1720 cm^{-1} appeared in the spectrum of the org-ATP, verifying KH-570 had been modified on the ATP nanorods. After polymerization, the two peaks around 2860 and 2930 cm^{-1} in the spectrum of the ATP/PAA hydrogels became stronger, and the C═O stretch band of the carboxyl group at 1710 cm^{-1}, stretch of C−O, and deformation vibration of OH at about 1400 cm^{-1} appeared.[53] The results indicated that PAA had been successfully grafted onto ATP through copolymerization.

The SEM image (Figure 7) revealed that the ATP nanorods were completely implanted into the PAA matrices, also indicating that PAA was successfully grafted onto the ATP nanorods to form the cross-linked ATP/PAA nanocomposite hydrogels.

Adsorption Properties of ATP/PAA Hydrogel A2-5 Toward Heavy Metal Ions. The competitive adsorption of the heavy metal ions (Pb^{2+}, Cd^{2+}, Zn^{2+}, Ni^{2+}, and Cu^{2+}) on ATP/PAA hydrogel A2-5 was evaluated, and the results are summarized in Figure 8. In good agreement with the previous

dx.doi.org/10.1021/sc400321v | ACS Sustainable Chem. Eng. 2014, 2, 643−651

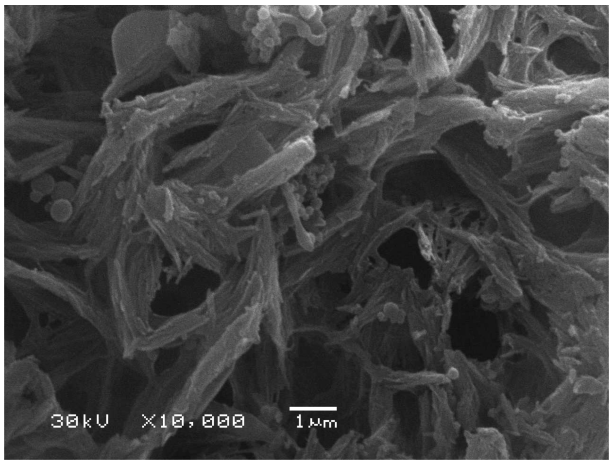

Figure 7. SEM image of the ATP/PAA hydrogel A-5.

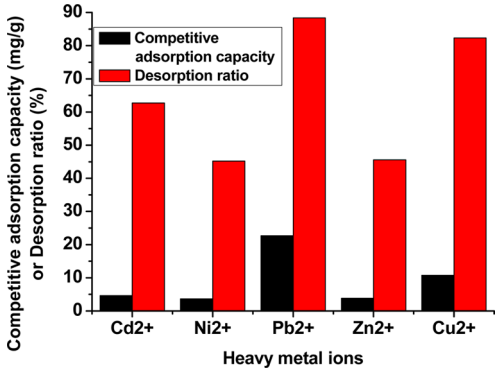

Figure 8. Competitive adsorption capacities and desorption ratios of the A2-5 to different heavy metal ions.

reports,[54,55] the carboxyl group-containing ATP/PAA hydrogel A2-5 exhibited better adsorption selectivity toward the Pb^{2+} ion with an adsorption capacity of 22.67 mg/g. The adsorption selectivity might be explained by the difference in the metal ion properties such as ionic radius, electronegativity, and ionization potential.[56,57] Furthermore, the corresponding desorption ratio in 1.0 mol/L HCl aqueous solution after 3 h reached the highest value of 88.4%, indicating its reusability.

Adsorption Properties of ATP/PAA Hydrogel A2-5 Toward Pb^{2+} Ion. Accurately weighed A2-5 (0.10 g) was added into 50 mL of a 100 mg/L Pb^{2+} solution and stirred in a magnetic stirrer for 0.5, 1, 1.5, 2.0, 2.5, 3.0, 4.0, or 5.0 h, respectively. The remaining Pb^{2+} concentration was detected with FAAS to calculate the adsorption capacity of A2-5 to Pb^{2+} as a function of the adsorption time, as shown in Figure 9.

One can obviously observe three stages in the whole adsorption process. The absorption of the Pb^{2+} ion onto A2-5 was very fast in the first 0.5 h, which indicated that the Pb^{2+} ion permeated into the outer surface of A2-5 through film diffusion. In the process, the carboxylic groups acted as a bidentate chelate coordinate to Pb^{2+} in the complex (Scheme 2),[58] so the adsorbed Pb^{2+} ions acted as the ionic cross-linker.[51] As a result, the difussion of Pb^{2+} ions into the inner area of the nanocomposite hydrogel adsorbent was hindered. Then the adsorption decreased slowly, implying that the migration of the Pb^{2+} ion was driven by the film diffusion together with the intraparticle diffusion and reached saturation in about 4 h due to the slowdown of both diffusion mechanisms.[59]

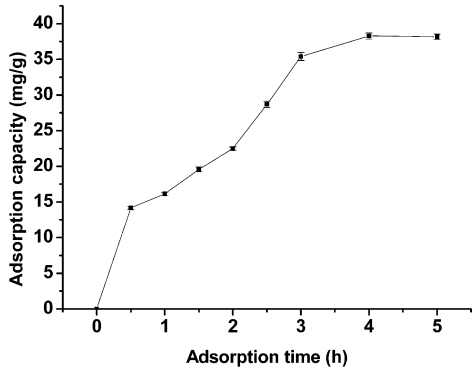

Figure 9. Adsorption capacity of A2-5 to Pb^{2+} ion as a function of adsorption time.

Scheme 2. Possible Chelating Structure Formed by the Adsorption of Pb^{2+} on the Carboxyl Group-Containing Hydrogel Adsorbent

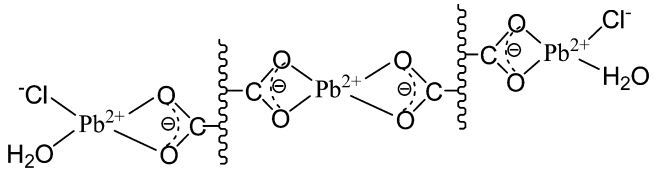

Then the effect of the pH values of the adsorption media on the adsorption capacity was investigated by stirring A2-5 (0.1 g) in 50 mL of 100 mg/L Pb^{2+} solutions with different pH values for 4 h. The calculated adsorption capacity of A2-5 to the Pb^{2+} ion as a function of pH value is shown by Figure 10. One can

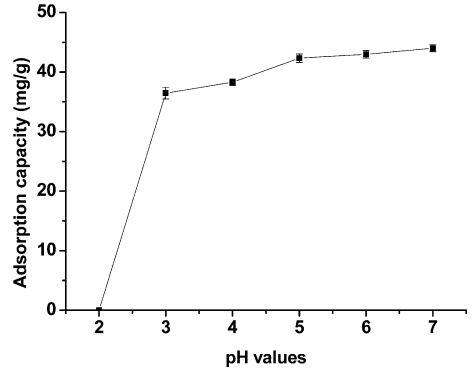

Figure 10. Adsorption capacity of A2-5 to Pb^{2+} ion as a function of pH value.

see that the adsorption capacity of A2-5 toward the Pb^{2+} ion was zero when pH was lower than 2 and increased rapidly before pH reached 3, followed by a slow increase from pH 3 to 5, and then reached a plateau of 42.32 mg/g when pH is increased to 5. In order to get a relatively higher adsorption capacity to Pb^{2+} and avoid the hydrolysis of Pb^{2+} at the same time, the adsorption of A2-5 to Pb^{2+} is better to be carried out in pH 5 media.

Desorption of Pb^{2+} Ion. After the Pb^{2+} ion was adsorbed and saturated at pH 5 for 24 h, the Pb^{2+} ion-adsorbed specimens were filtered and put into 50 mL of aqueous HCl solutions of 0.50, 0.75, 1.00, 1.25, and 1.50 mol/L, respectively. After being stirred for 1 h, the concentrations of the eluted ions in the upper liquid were also measured by AAS. The desorption ratio

dx.doi.org/10.1021/sc400321v | ACS Sustainable Chem. Eng. 2014, 2, 643−651

(mass ratio of the eluted ion to adsorbed ion) of the Pb^{2+} ion from ATP/PAA hydrogel A2-5 as a function of the concentration of an HCl aqueous solution is shown in Figure 11. The highest desorption ratio (89.9%) of the Pb^{2+} ion from A2-5 was obtained with a 0.50 mol/L HCl solution as eluant.

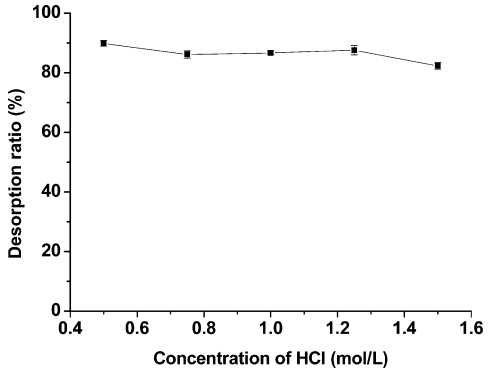

Figure 11. Desorption rate of Pb^{2+} ion from A2-5 by HCl solutions with different concentrations.

The Pb^{2+} ion-adsorbed specimens were filtrated and put into 50 mL of 0.50 mol/L HCl aqueous solutions and stirred for 20, 40, 60, 80, 100, and 120 min, respectively. The eluted Pb^{2+} ion from A2-5 was determined by FAAS to calculate the desorption ratio of as a function of desorption time, as shown in Figure 12. The desorption of Pb^{2+} ion from A2-5 in a 0.50 mol/L HCl solution reached equilibrium in about 100 min with the desorption ratio as high as 98.2%.

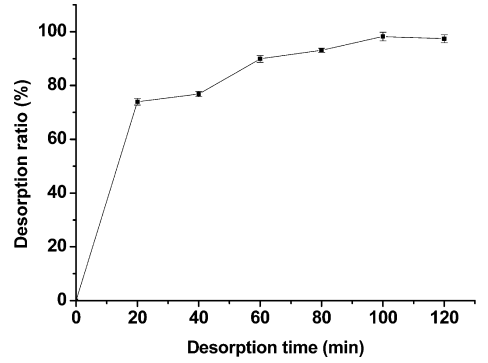

Figure 12. Desorption ratio of Pb^{2+} ion from A2-5 as a function of desorption time.

Reusability of ATP/PAA A2-5. In order to evaluate the continued regeneration and reuse of the ATP/PAA A2-5 adsorbent, the adsorption capacity for Pb^{2+} and desorption efficacy from the first cycle through cycle 10 were investigated with the following process. After 0.1 g of accurately weighed A2-5 was added into 50 mL of a 100 mg/L Pb^{2+} solution of pH 5 and stirred for 4 h, the remaining Pb^{2+} concentration in the solution was measured by FAAS to calculate its adsorption capacity, while the nanocomposite hydrogel adsorbent saturated with Pb^{2+} was filtrated and eluted with 50 mL of a 0.5 mol/L aqueous HCl solution for 2 h. Thus, a complete cycle of adsorption−desorption was finished. The eluted A2-5 adsorbent was charged another nine times with the adsorption−desorption cycle, and the adsorption capacity and desorption ratio from the first cycle through cycle 10 were calculated and are exhibited in Figure 13. After 10 cycles of adsorption−desorption, the adsorption capacity and desorption ratio remained more than 99% and 96%, compared with those of the first cycle, indicating an excellent reusability of the nanocomposite hydrogel adsorbent A2-5.

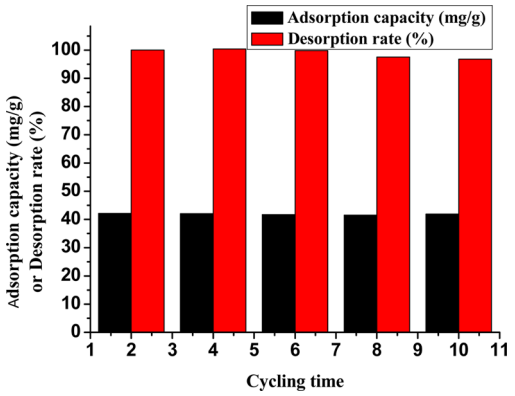

Figure 13. Reusability of nanocomposite hydrogel adsorbent A2-5.

CONCLUSIONS

Attapulgite nanorods (ATP) were modified by KH-570 in liquid paraffin with Span-80 and Tween-60 as dispersing agenst. Compared to the traditional process, the obtained intermediate can be directly used in the next step without any treatment because its reaction medium is the same as that of the further polymerization. Then the functional org-ATP nanorods were used as the unique cross-linker in inverse suspension polymerization to form the 3-dimensional cross-linking network structure of the ATP/PAA nanocomposite hydrogels.

The orthogonal experiment results indicated that the oil−water ratio was the most important factor, and the ATP/PAA hydrogels can be obtained only when the oil−water ratio is 3:1. Meanwhile, it was concluded that A2 is the best formula. A series of single factor experiments were carried out to investigate the effects of the mass ratio of AA to ATP on the products, and A2-5 was identified as an optimal formula with its overall good performance and low cost.

The ATP/PAA hydrogel A2-5 showed good adsorption selectivity toward the Pb^{2+} ion with saturated adsorption capacity of 42.32 mg/g at the optimal media (pH 5.0) within 4 h. The adsorbed Pb^{2+} ion could be completely desorbed from the adsorbent with 0.50 mol/L HCl aqueous solution as eluant in 100 min. After 10 cycles of adsorption−desorption, the adsorption capacity and desorption rate did not change. All these results indicate that A2-5 has an excellent reproducibility as a low-cost selective adsorbent for Pb^{2+} ion.

ASSOCIATED CONTENT

Supporting Information

The $L_{16}(4^5)$ Orthogonal Experiment and digital photos of the products. This material is available free of charge via the Internet at http://pubs.acs.org.

AUTHOR INFORMATION

Corresponding Author

*E-mail: pliu@lzu.edu.cn. Tel./Fax: 86-931-8912582.

Notes

The authors declare no competing financial interest.

REFERENCES

(1) Sonune, A.; Ghate, R. Developments in wastewater treatment methods. *Desalination* **2004**, *167*, 55−63.
(2) Fu, F. L.; Wang, Q. Removal of heavy metal ions from wastewaters: A review. *J. Environ. Manage.* **2011**, *92*, 407−418.
(3) Dabrowski, A.; Hubicki, Z.; Podkoscienlny, P.; Robens, E. Selective removal of the heavy metal ions from waters and industrial wastewaters by ion-exchange method. *Chemosphere* **2004**, *56*, 91−106.
(4) Schexnailder, P. Nanocomposite polymer hydrogels. *Colloid Polym. Sci.* **2009**, *287*, 1−11.
(5) Messing, R.; Schmidt, A. M. Perspectives for the mechanical manipulation of hybrid hydrogels. *Polym. Chem.* **2011**, *2*, 18−32.
(6) Kabiri, K.; Omidian, H.; Zohuriaan-Mehr, M. J.; Doroudiani, S. Superabsorbent hydrogel composites and nanocomposites: A review. *Polym. Compos.* **2011**, *32*, 277−289.
(7) Shibayama, M. Structure-mechanical property relationship of tough hydrogels. *Soft Matter* **2012**, *8*, 8030−8038.
(8) Pan, B. J.; Pan, B. C.; Zhang, W. M.; Lv, L.; Zhang, Q. X.; Zheng, S. R. Development of polymeric and polymer-based hybrid adsorbents for pollutants removal from waters. *Chem. Eng. J.* **2009**, *151*, 19−29.
(9) Jang, S. H.; Min, B. G.; Jeong, Y. G.; Lyoo, W. S.; Lee, S. C. Removal of lead ions in aqueous solution by hydroxyapatite/polyurethane composite foams. *J. Hazard. Mater.* **2008**, *152*, 1285−1292.
(10) Wang, X. H.; Zheng, Y.; Wang, A. Q. Fast removal of copper ions from aqueous solution by chitosan-g-poly(acrylic acid)/palygorskite composites. *J. Hazard. Mater.* **2009**, *168*, 970−977.
(11) Dinu, M. V.; Dragan, E. S. Evaluation of Cu^{2+}, Co^{2+} and Ni^{2+} ions removal from aqueous solution using a novel chitosan/clinoptilolite composite: Kinetics and isotherms. *Chem. Eng. J.* **2010**, *160*, 157−163.
(12) Paulino, A. T.; Belfiore, L. A.; Kubota, L. T.; Muniz, E. C.; Almeida, V. C.; Tambourgi, E. B. Effect of magnetite on the adsorption behavior of Pb(II), Cd(II), and Cu(II) in chitosan-based hydrogels. *Desalination* **2011**, *275*, 187−196.
(13) Tirtom, V. N.; Dincer, A.; Becerik, S.; Aydemir, T.; Celik, A. Comparative adsorption of Ni(II) and Cd(II) ions on epichlorohydrin crosslinked chitosan−clay composite beads in aqueous solution. *Chem. Eng. J.* **2012**, *197*, 379−386.
(14) Googerdchian, F.; Moheb, A.; Emadi, R. Lead sorption properties of nanohydroxyapatite−alginate composite adsorbents. *Chem. Eng. J.* **2012**, *200*, 471−479.
(15) Singh, V.; Pandey, S.; Singh, S. K.; Sanghi, R. Removal of cadmium from aqueous solutions by adsorption using poly(acrylamide) modified guar gum−silica nanocomposites. *Sep. Pur. Technol.* **2009**, *67*, 251−261.
(16) Anirudhan, T. S.; Ramachandran, M. Synthesis and characterization of amidoximated polyacrylonitrile/organobentonite composite for Cu(II), Zn(II), and Cd(II) adsorption from aqueous solutions and industry wastewaters. *Ind. Eng. Chem. Res.* **2008**, *47*, 6175−6184.
(17) An, F. Q.; Gao, B. J. Chelating adsorption properties of PEI/SiO_2 for plumbum ion. *J. Hazard. Mater.* **2007**, *145*, 495−500.
(18) Qiu, J. Y.; Wang, Z. Y.; Li, H. B.; Xu, L.; Peng, J.; Zhai, M. L.; Yang, C.; Li, L. Q.; Wei, G. S. Adsorption of Cr(VI) using silica-based adsorbent prepared by radiation induced grafting. *J. Hazard. Mater.* **2009**, *166*, 270−276.
(19) Shao, D. D.; Jiang, Z. Q.; Wang, X. K.; Li, J. X.; Meng, Y. D. Plasma induced grafting carboxymethyl cellulose on multiwalled carbon nanotubes for the removal of UO_2^{2+} from aqueous solution. *J. Phys. Chem. B* **2009**, *113*, 860−864.
(20) Zhao, Y. J.; Chen, Y.; Li, M. S.; Zhou, S. Y.; Xue, A. L.; Xing, W. H. Adsorption of Hg^{2+} from aqueous solution onto polyacrylamide/attapulgite. *J. Hazard. Mater.* **2009**, *171*, 640−646.
(21) Liu, P.; Wang, T. M. Adsorption properties of hyperbranched aliphatic polyester grafted attapulgite towards heavy metal ions. *J. Hazard. Mater.* **2007**, *149*, 75−79.
(22) Liu, P.; Guo, J. S. Polyacrylamide grafted attapulgite (PAM-ATP) via surface-initiated atom transfer radical polymerization (SI-ATRP) for removal of Hg(II) ion and dyes. *Colloid Surf., A* **2006**, *282*, 498−503.
(23) Takafuji, M.; Ide, S.; Ihara, H.; Xu, Z. H. Preparation of poly(1-vinylimidazole) grafted magnetic nanoparticles and their applications for the removal of metal ions. *Chem. Mater.* **2004**, *16*, 1977−1983.
(24) Mandavian, A. R.; Mirrahimi, M. A. S. Efficient separation of heavy metal cations by anchoring polyacrylic acid on superparamagnetic magnetite nanoparticles through surface modification. *Chem. Eng. J.* **2010**, *159*, 264−271.
(25) Song, J.; Kong, H.; Jang, J. Adsorption of heavy metal ions from aqueous solution by polyrhodanine-encapsulated magnetic nanoparticles. *J. Colloid Interface Sci.* **2011**, *359*, 505−511.
(26) Pang, Y.; Zeng, G. M.; Tang, L.; Zhang, Y.; Liu, Y. Y.; Lei, X. X.; Li, Z.; Zhang, J. C.; Liu, Z. F.; Xiong, Y. Q. Preparation and application of stability enhanced magnetic nanoparticles for rapid removal of Cr(VI). *Chem. Eng. J.* **2011**, *175*, 222−227.
(27) Zhao, Q. C.; Cao, T. Polyacrylonitrile/silica nanospheres with three- dimensional interpenetrating network structure and their application for removal of Pb(II) from water. *Ind. Eng. Chem. Res.* **2012**, *51*, 4952−4957.
(28) Grøtli, M.; Rademan, J.; Groth, T.; Lubell, W. D.; Miranda, L. P.; Meldal, M. Surfactant mediated cationic and anionic suspension polymerization of PEG-based resins in silicon oil: Beaded SPOCC 1500 and POEPOP 1500. *J. Comb. Chem.* **2001**, *3*, 28−33.
(29) Schubert, U. Nano-scale structures of sol-gel materials. *Chem. Mater.* **2001**, *13*, 3487−3494.
(30) Haraguchi, K.; Takehisa, T. Nanocomposites hydrogels: A unique organic-inorganic network structure with extraaodinary mechanical, optical, and swelling/de-swelling properties. *Adv. Mater.* **2002**, *24*, 1120−1124.
(31) Hu, Y.; Zhou, S. X.; Wu, L. M. Surface mechanical properties of transparent poly(methyl methacrylate)/zirconia nanocomposites prepared by in situ bulk polymerization. *Polymer* **2009**, *50*, 3609−3616.
(32) Haraguchi, K. Synthesis and properties of soft nanocomposite materials with novel organic/inorganic network structures. *Polym. J.* **2011**, *43*, 223−241.
(33) Herrera, N. N.; Letoffe, J.-M.; Putaux, J.-L.; David, L.; Bourgeat-Lami, E. A first step toward the elaboration of water-based polymer/clay nanocomposites. *Langmuir* **2004**, *20*, 1564−1571.
(34) Herrera, N. N.; Letoffe, J.-M.; Reymond, J. P.; Bourgeat-Lami, E. Silylation of laponite clay particles with monofunctional and trifunctional vinyl alkoxysilanes. *J. Mater. Chem.* **2005**, *15*, 863−871.
(35) Zhou, T. H.; Ruan, W. H.; Mai, Y. L.; Rong, M. Z.; Zhang, M. Q. Performance improvement of nano-silica/polypropylene composites through in-situ crosslinking approach. *Compos. Sci. Technol.* **2008**, *68*, 2858−2863.
(36) Wang, X.; Pan, J.; Guan, W.; Dai, J.; Zou, X.; Yan, Y.; Li, C.; Hu, W. Selective removal of 3-chlorophenol from aqueous solution using surface molecularly imprinted microspheres. *J. Chem. Eng. Data* **2011**, *56*, 2793−2801.
(37) Isoda, K.; Kuroda, K. Grafting of -methacryloxypropylsilyl groups in the interlayer space of layered polysilicate magadiite and the copolymerized products with methylmethacrylate. *Chem. Mater.* **2000**, *12*, 1702−1707.
(38) Ni, W. S.; Wu, S. P.; Ren, Q. Preparation and characterization of silanized TiO_2 nanoparticles and their application in toner. *Ind. Eng. Chem. Res.* **2012**, *51*, 13157−13163.
(39) Guo, Z. H.; Pereira, T.; Choi, O.; Wang, Y.; Hahn, H. T. Surface functionalized alumina nanoparticle filled polymeric nanocomposites with enhanced mechanical properties. *J. Mater. Chem.* **2006**, *16*, 2800−2808.
(40) Zhu, X. X.; Su, N.; Li, H. B.; Liu, X. H.; Li, Y. Synthesis and characterization of spherical polymer brushes. *Mater. Lett.* **2011**, *65*, 2816−2819.
(41) Liu, P.; Liu, Y. S.; Su, Z. X. Competitive adsorption of some heavy metal ions on modified polymers. *Ind. Eng. Chem. Res.* **2006**, *45*, 2255−2260.

(42) Ruiz, J.; Mantecon, A.; Cadiz, V. Synthesis and properties of hydrogels from poly (vinyl alcohol) and ethylenediaminetetraacetic dianhydride. *Polymer* **2001**, *42*, 6347−6354.
(43) Du, M. C.; Song, W. X.; Cui, Y.; Yang, Y.; Li, J. B. Fabrication and biological application of nano-hydroxyapatite (nHA)/alginate (ALG) hydrogel as scaffolds. *J. Mater. Chem.* **2011**, *21*, 2228−2236.
(44) Marandi, G. B.; Hariri, S.; Mahdavinia, G. R. Effect of hydrophobic monomer on the synthesis and swelling behaviour of a collagen-graft-poly[(acrylic acid)-co-(sodium acrylate)] hydrogel. *Polym. Int.* **2009**, *58*, 227−235.
(45) Bronich, T. K.; Vinogradov, S. V.; Kabanov, A. V. Interaction of nanosized copolymer networks with oppositely charged amphiphilic molecules. *Nano Lett.* **2001**, *1*, 535−540.
(46) Wu, S. N.; Li, H.; Chen, J. P.; Lam, K. Y. Modeling investigation of hydrogel volume transition. *Macromol. Theory Simul.* **2003**, *13*, 13−29.
(47) Lu, H.; Shen, H.; Song, Z.; Shing, K. S.; Tao, W.; Nutt, S. Rod-like silicate-epoxy nanocomposites. *Macromol. Rapid Commun.* **2005**, *26*, 1445−1450.
(48) Jana, N. R.; Gearheart, L.; Murphy, C. J. Wet chemical synthesis of high aspect ratio cylindrical gold nanorods. *J. Phys. Chem. B* **2001**, *105*, 4065−4067.
(49) Nathanael, A. J.; Mangalaraj, D.; Chen, P. C.; Ponpandian, N. enhanced mechanical strength of hydroxyapatite nanorods reinforced with polyethylene. *J. Nanopart. Res.* **2011**, *13*, 1841−1853.
(50) Ljungberg, N.; Cavaille, J. Y.; Heux, L. Nanocomposites of isotactic polypropylene reinforced with rod-like cellulose whiskers. *Polymer* **2006**, *47*, 6285−6292.
(51) Kuo, C. K.; Ma, P. X. Ionically crosslinked alginate hydrogels as scaffolds for tissue engineering: Part 1. Structure, gelation rate and mechanical properties. *Biomaterials* **2001**, *22*, 511−521.
(52) Wang, Y.; Zeng, L.; Ren, X.; Song, H.; Wang, A. Removal of methyl violet from aqueous solutions using poly (acrylic acid-co-acrylamide)/attapulgite composite. *J. Environ. Sci.* **2010**, *22*, 7−14.
(53) Wu, N. Q.; Fu, L.; Aslam, M.; Wong, K. C.; Dravid, V. P. Interaction of fatty acid monolayers with cobalt nanoparticles. *Nano Lett.* **2004**, *4*, 383−386.
(54) Chowdhury, P.; Pandit, S. K.; Mandal, B. Preparation and characterization of silanized silica gel-supported poly(acrylic acid) network polymer and study of its analytical application as selective extractor for lead ion. *J. Appl. Polym. Sci.* **2008**, *110*, 475−480.
(55) Ahmetli, G.; Yel, E.; Deveci, H.; Bravo, Y.; Bravo, Z. Investigation of Pb(II) adsorption onto natural and synthetic polymers. *J. Appl. Polym. Sci.* **2012**, *125*, 716−724.
(56) Lao, C.; Zelendon, Z.; Gamisans, X.; Sole, M. Sorption of Cd(II) and Pb(II) from aqueous solutions by a low-rank coal (leonardite). *Sep. Purif. Technol.* **2005**, *45*, 79−85.
(57) Demir-Cakan, R.; Baccile, N.; Antonietti, M.; Titirici, M.-M. Carboxylate-rich carbonaceous materials via one-step hydrothermal carbonization of glucose in the presence of acrylic acid. *Chem. Mater.* **2009**, *21*, 484−490.
(58) Liang, X.; Su, Y. B.; Yang, Y.; Qin, W. W. Separation and recovery of lead from a low concentration solution of lead(II) and zinc(II) using the hydrolysis production of poly styrene-co-maleic anhydride. *J. Hazard. Mater.* **2012**, *203−204*, 183−187.
(59) Chen, H.; Wang, A. Adsorption characteristics of Cu(II) from aqueous solution onto poly(acrylamide)/attapulgite composite. *J. Hazard. Mater.* **2009**, *165*, 223−231.